

An *in Situ* Fourier Transform Infrared Study of Formic Acid Adsorption on a Polycrystalline Silver Catalyst

Graeme J. Millar, James B. Metson, Graham A. Bowmaker, and Ralph P. Cooney¹

Department of Chemistry, University of Auckland, Private Bag 92019, Auckland, New Zealand

Received October 21, 1993; revised December 10, 1993

Infrared spectra are reported for the adsorption of formic acid on a polycrystalline silver catalyst after various degrees of oxidation. Three distinct chemisorbed species were identified, two of which corresponded to adsorbed formate on Ag(110) and Ag(111) crystal planes and the other to adsorbed formate on a silver site modified by the presence of subsurface oxygen. Moreover, it was discovered that subsurface oxygen species were primarily located in the vicinity of grain boundary defects. Desorption profiles suggested that coadsorbed oxygen moieties could destabilize chemisorbed formate. Because of the invariance in infrared band positions associated with formate species, regardless of whether or not neighbouring atomic oxygen species were present, a kinetic stabilization mechanism is proposed. The pivotal role of subsurface oxygen species found in the region of grain boundaries, in the mechanism for the selective oxidation of methanol to formaldehyde, is emphasised. © 1994 Academic Press, Inc.

INTRODUCTION

Silver catalysts are used extensively for both the production of ethylene oxide by partial oxidation of ethylene and formation of formaldehyde from the partial oxidation of methanol. In the case of ethylene epoxidation the catalyst usually consists of silver particles on α -Al₂O₃, whereas electrolytic silver is commonly utilised for methanol oxidation. Due to the worldwide importance of these processes, considerable effort has been devoted to the elucidation of the reaction mechanisms involved (1–4). One of the most intriguing aspects of silver chemistry has proved to be the complex adsorption behaviour of oxygen. Exposure of an Ag(110) single crystal resulted in the identification of both adsorbed molecular and atomic oxygen species (5), which desorbed at 190 K and 590 K, respectively. Campbell (6) also observed molecular and atomic oxygen species on Ag(111). However, subsurface oxygen species were also apparent in this study. The concentration of subsurface species is usually enhanced by high-temperature treatment of silver in the presence of oxygen

(7). In relation to this effect Grant and Lambert (8, 9) noted the appearance of an unusually strongly bound molecular oxygen species ($T_{\text{max}} = 380$ K) on an Ag(111) surface, which was associated with the presence of subsurface oxygen. Wu *et al.* (10) proposed that the formation of subsurface oxygen was related to the presence of defect sites on the silver surface and, moreover, these defect sites were concluded to be responsible for the stabilization of molecular oxygen species.

Infrared spectroscopy has proved to be a very powerful method for the study of adsorbates on catalyst surfaces (11), especially as investigations are not limited to the UHV conditions necessary for electron spectroscopic techniques. Wang *et al.* (12, 13) identified molecular and atomic oxygen species on a polycrystalline silver catalyst using RAIRS. In addition they postulated the existence of two distinct molecular oxygen species, one of which was associated with defect sites on the surface. Force and Bell (14–16) have also conducted a study of the ethylene oxidation reaction on supported silver catalysts by transmission infrared spectroscopy. However, no detailed infrared investigations have been reported concerning the effect of oxygen treatment of silver catalysts upon the adsorption of simple molecules (such as HCOOH, CO₂, C₂H₂, HCHO, CH₃OH, etc.) which are relevant to both the ethylene epoxidation and methanol oxidation reactions.

Consequently this paper reports an *in situ* FT-IR study of formic acid (HCOOH) on a model Ag/SiO₂ catalyst treated to achieve various degrees of oxidation.

EXPERIMENTAL

Usually model silver catalysts have been prepared by impregnation of a support material with an aqueous solution of silver nitrate (14–18). However, in the present case it is desirable to design a catalyst consisting of very small particles, which should expose both high and low index planes, and be rich in defect structures, such as grain boundaries. Previously it has been shown that if silica was impregnated with copper(II) acetate monohy-

¹ To whom correspondence should be addressed.

drate this would ultimately result in formation of a catalyst consisting of polycrystalline copper metal particles of average size <5 nm after reduction in hydrogen (19, 20). Therefore a silica-supported silver catalyst was prepared in the following manner. Silica (Cab-O-Sil M5, $200 \text{ m}^2 \text{ g}^{-1}$) was impregnated with an aqueous solution of silver (I) acetate (Aldrich, 99.999%) and subsequently dried at 383 K for 5 h. A self-supporting disc (ca. 18 mm diameter) was formed by pressing ca. 75 mg of powder at minimal pressure. Following placement of the catalyst in an *in situ* FT-IR cell capable of operating at temperatures between 77 and 773 K, (21) the sample was calcined in O_2 ($50 \text{ cm}^3 \text{ min}^{-1}$) at 573 K for 1.5 h, and then reduced in hydrogen ($75 \text{ cm}^3 \text{ min}^{-1}$) which had firstly been purified by passage through a deoxo unit and a molecular sieve, at 623 K for 17 h. Finally the reduced catalyst which contained ca. 5 wt% silver on silica was evacuated in order to desorb any residual hydrogen and water species in the system.

Reoxidation of the silver surface was accomplished by either exposure to N_2O (NZIG, 99.9%) or O_2 (NZIG, 99.6%) for varying periods of time at 473 K.

FT-IR spectra were obtained using a Digilab FTS-60 Fourier Transform spectrometer equipped with an MCT detector. Spectra were recorded at 4 cm^{-1} resolution and averaged over 64 scans. Peak deconvolution was achieved by use of Spectracalc software (Galactic Industries). Peak height was taken to be a good measure of the absorbance of any one band. In order for this approximation to be valid the FWHM of a particular band was kept constant throughout all curve-fit procedures.

A typical experiment involved dosing formic acid onto the catalyst at 273 K followed by evacuation of the system to high vacuum at that same temperature. Subsequently the sample was heated linearly at 6 K min^{-1} under rapid pumping, and spectra were then acquired as a function of catalyst temperature. Desorption profiles were constructed by relating the peak absorbance of an individual formate band as a function of catalyst temperature. Determination of the temperature at which the maximum rate of desorption occurred (T_{max}) was performed in the same manner as described previously (21).

RESULTS

Adsorption of Formic Acid on a Reduced Catalyst

Figure 1a shows the spectrum obtained after exposure of a reduced silver catalyst (Ag/SiO_2) to formic acid at 295 K. Bands were evident at 2941, 1722, 1389, and ca. 1359 cm^{-1} which could readily be assigned to the presence of formic acid molecules physisorbed to the silica support (22). However, the broad maximum detected at ca. 1564 cm^{-1} cannot be attributed to any reported species on silica. McQuillan and Pope (23) used Raman spectroscopy

to study formate ion adsorption on silver. They identified a band at 1550 cm^{-1} which was assigned to the $\nu_{\text{as}}(\text{COO})$ mode of formate species adsorbed on silver particles. Therefore it is proposed that chemisorbed formate on silver was found on the surface of the reduced catalyst. This conclusion was reinforced by the fact that when the temperature was increased to 341 K (Fig. 1c) causing substantial desorption of physisorbed formic acid species, peaks were revealed at 2941, 2814, ca. 1585, 1378 (sh), and 1339 cm^{-1} . From the Raman data of McQuillan and Pope (23) and the EELS results of Sexton and Madix (24) for formic acid adsorption on $\text{Ag}(110)$, we can ascribe the bands to the following modes of adsorbed formate on silver: 2814 cm^{-1} , $\nu(\text{CH})$; 1585 cm^{-1} , $\nu_{\text{as}}(\text{COO})$; 1378 (sh), $\delta(\text{CH})$; and 1339 cm^{-1} , $\nu_{\text{s}}(\text{COO})$. The remaining maximum at 2941 cm^{-1} can be assigned by analogy to previous data concerning the adsorption of formic acid on copper. Hayden *et al.* (25, 26) attributed a band at 2950 cm^{-1} to a combination mode [$\nu_{\text{as}}(\text{COO}) + \delta(\text{CH})$] of copper formate species. A similar combination of peaks in this silver system would be expected to produce a band at ca. 2963 cm^{-1} which was in agreement with the position of the observed maximum (2941 cm^{-1}).

Raising the catalyst temperature (Figs. 1d–i) caused the concomitant diminishment of all peaks associated with silver formate species. As shown previously (21), a plot of the absorbance of any of the formate vibrational modes as a function of catalyst temperature should allow the temperature at which the maximum rate of desorption occurs (denoted as T_{max}) to be calculated. However, it was apparent from the spectra displayed in Fig. 1 that the profiles at ca. 2814 and 1564 cm^{-1} were asymmetric in nature. This behaviour implied that more than one formate species resided on the silver surface. Indeed curve-fitting (using the assumption that the peaks were 100% Gaussian) of the $\nu(\text{CH})$ and $\nu_{\text{as}}(\text{COO})$ profiles obtained in Fig. 1c suggested the presence of two distinct formate species (Fig. 2). Subbands at 2814 and 1586 cm^{-1} are ascribed to vibrations of species "A" and subbands at 2843 and 1545 cm^{-1} to modes of species "B".

Figure 3 shows the relationships obtained by plotting not only the absorbance of the overall profile at ca. 1564 cm^{-1} assigned to the $\nu_{\text{as}}(\text{COO})$ mode for adsorbed formate on silver but also the absorbance of the relevant subbands. Notably the profile relating the overall band intensity with catalyst temperature did not display the shape of an ideal first order desorption isotherm (21). This evidence was in accordance with the observed asymmetry of the $\nu_{\text{as}}(\text{COO})$ mode which suggested the presence of more than one species. Indeed the subband at 1586 cm^{-1} showed typical desorption characteristics, and it was calculated that the maximum rate of desorption occurred at a temperature (T_{max}) of 421 K. This value was similar to that reported by Barteau *et al.*

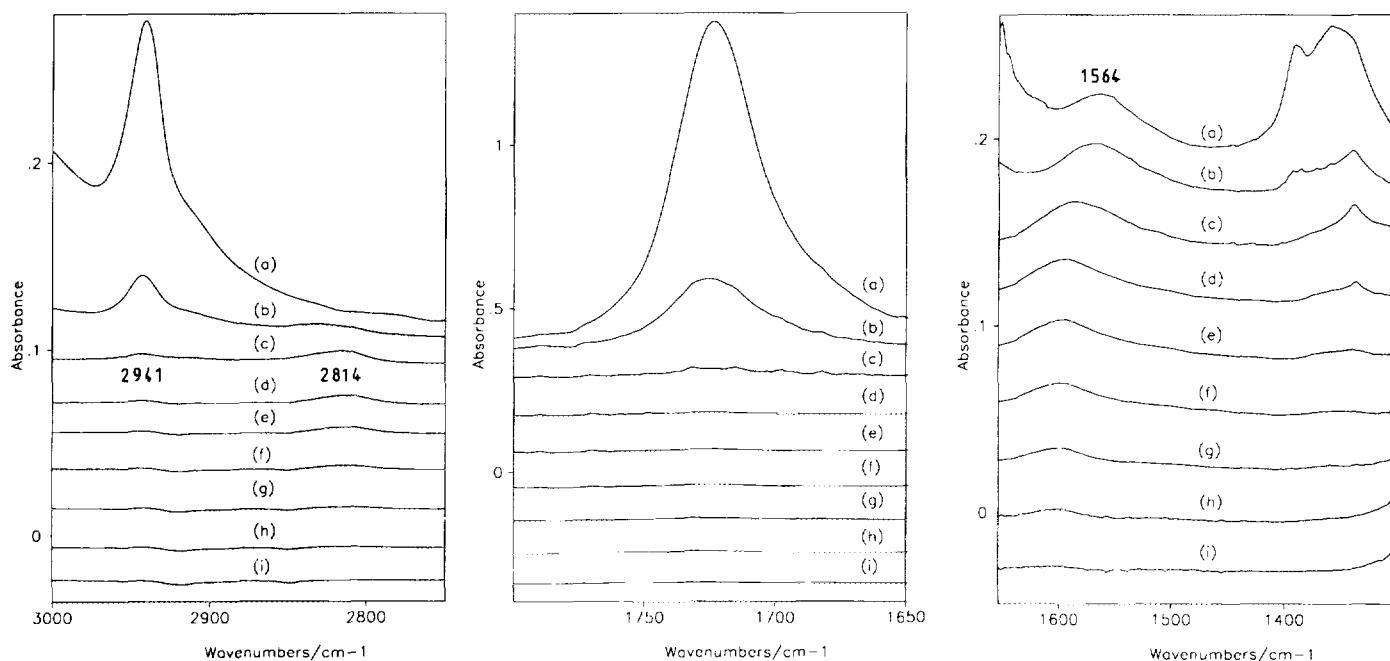


FIG. 1. A reduced silver catalyst was exposed to formic acid vapour at 295 K, and then subsequently heated linearly under vacuum conditions. Infrared spectra were recorded as a function of catalyst temperature (a) 295, (b) 317, (c) 341, (d) 388, (e) 400, (f) 412, (g) 424, (h) 436, and (i) 460 K.

(27) of 410 K which was attributed to the decomposition of formate on a clean silver metal single crystal. Stuve *et al.* (28) have also concluded that the reaction between formaldehyde and adsorbed oxygen on a Ag(110) surface

gave rise to a chemisorbed formate species which desorbed at a T_{\max} value of 410 K.

Significantly the desorption profile for the 1545 cm^{-1} subband did not show ideal behaviour. Indeed the profile

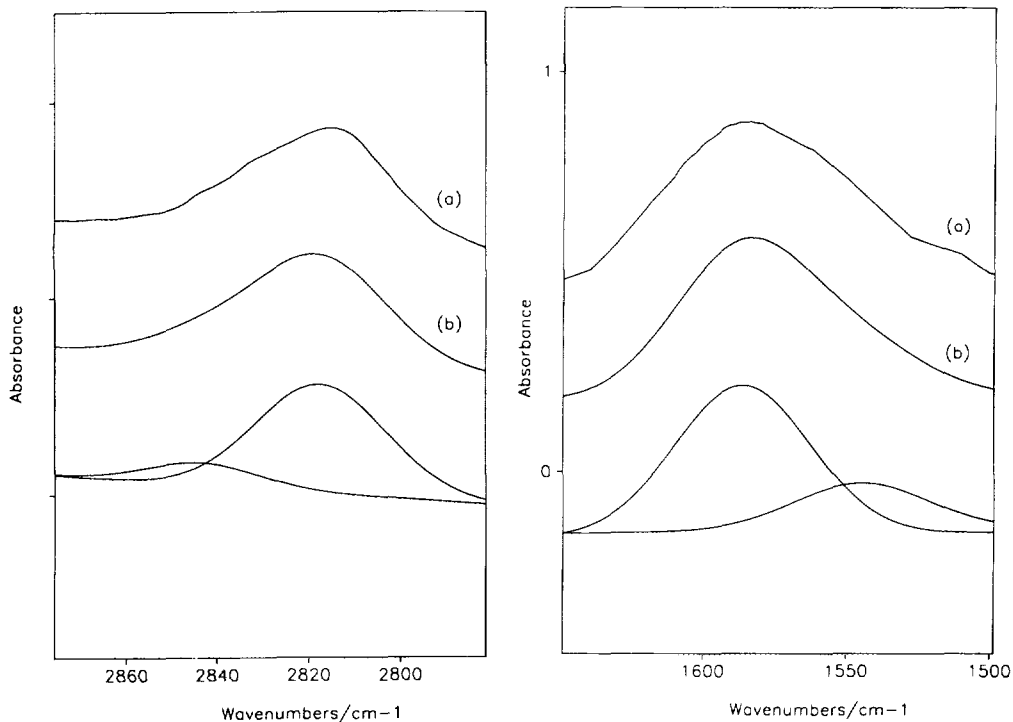


FIG. 2. Curve-fit analysis of the spectrum shown in Fig. 1c. (a) actual spectrum, (b) corresponding overall curve-fit. Remaining peaks are the calculated subbands.

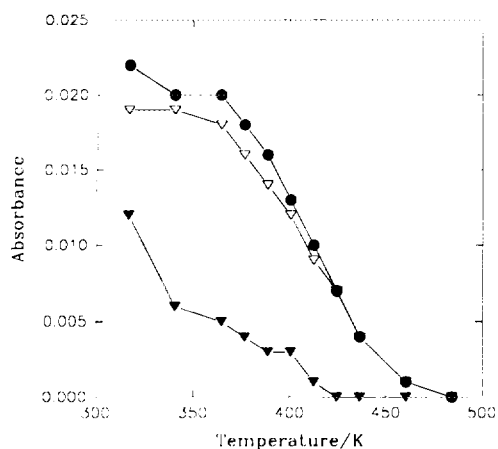


FIG. 3. Desorption profile obtained by monitoring the absorbance of the profile at ca. 1564 cm^{-1} (Fig. 1) and also the calculated subbands, as a function of catalyst temperature. (●) absorbance of overall profile due to $\nu_{\text{as}}(\text{COO})$ mode, (▽) absorbance of subband at 1586 cm^{-1} , and (▼) absorbance of subband at 1545 cm^{-1} .

can only be explained if it is assumed that three distinct species are present which give rise to the same infrared band positions, but differ substantially in desorption character. From the shape of the profile in Fig. 3 it can be estimated that the T_{max} values of these three species are in the range $340\text{--}350\text{ K}$, $385\text{--}400\text{ K}$, and $410\text{--}420\text{ K}$. Interestingly, Sault and Madix (29) demonstrated that the presence of coadsorbed oxygen destabilized formate species

on a silver surface. Temperature programmed reaction spectroscopy (TPRS) studies of formic acid coadsorbed with oxygen on $\text{Ag}(110)$ showed desorption states at 345 , 385 , and 410 K which correlate well with the T_{max} values observed in this study. Consequently it can be inferred that even after the reduction procedure used in this study, a small proportion of the silver surface was covered in adsorbed oxygen species.

Adsorption of Formic Acid on a Nitrous Oxide Pretreated Catalyst

When a reduced silver surface was contacted with N_2O at 273 K no detectable change in the adsorption behaviour of formic acid was noted. This observation was consistent with the conclusion of Tan *et al.* (30) that the decomposition of nitrous oxide on a silver (111) single crystal was a significantly activated process. Therefore a reduced silver catalyst (Ag/SiO_2) was exposed to nitrous oxide (13.3 kPa) for 2 h at 473 K . In broad terms, the same peaks typical of formate species chemisorbed to silver were evident at 2939 , ca. 2822 , ca. 1580 , 1377 (sh), and 1341 cm^{-1} . Sub-band analysis of the $\nu(\text{CH})$ and $\nu_{\text{as}}(\text{COO})$ modes (Fig. 4) revealed that although N_2O oxidation apparently did not affect the concentration of species "A" (subbands at 2821 and 1586 cm^{-1}) an enhancement in the proportion of species "B" (subbands at 2843 and 1548 cm^{-1}) was discerned. Increasing the catalyst temperature resulted in

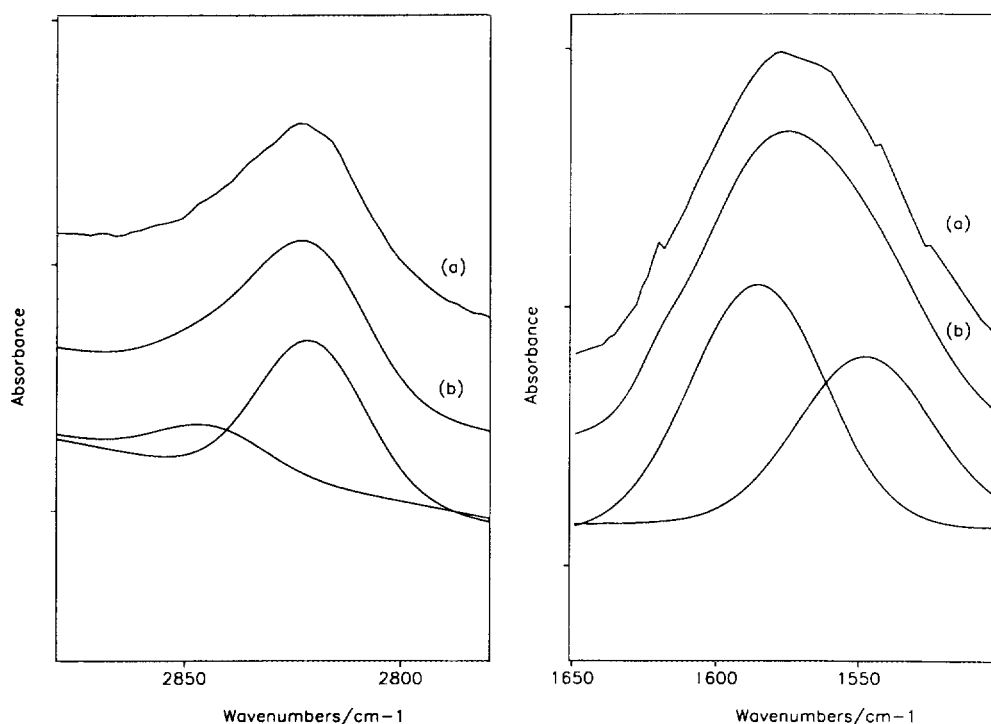


FIG. 4. Curve-fit analysis of the spectrum obtained by exposure of formic acid to a silver catalyst which had been reoxidised by nitrous oxide for 2 h at 473 K . (a) actual spectrum, (b) corresponding overall curve-fit. Remaining bands are the calculated subbands.

the desorption of formate species, and the relationship between the absorbance of the formate $\nu_{\text{as}}(\text{COO})$ vibration and catalyst temperature is shown in Fig. 5. It was concluded that N_2O pretreatment did not strongly influence either the concentration of species "A" (subband 1586 cm^{-1}) or the temperature at which the maximum rate of desorption occurred ($T_{\text{max}} = 420\text{ K}$). However, the quantity of species "B" exhibiting a maximum rate of desorption in the region $340\text{--}350\text{ K}$ increased dramatically. This behaviour indicated that the nitrous oxide treatment had partially oxidised the silver catalyst, depositing nucleophilic oxygen species on the surface which then promoted formic acid adsorption by abstraction of the acidic hydrogen (27).

Adsorption of Formic Acid on an Oxygen Pretreated Silver Catalyst

Reoxidation in 13.3 kPa O_2 for 5 min at 473 K. There exists a consensus of opinion that the oxidation rate of a silver surface by O_2 is considerably greater than the corresponding situation with N_2O (17, 31, 32). Thus a relatively mild oxidation of a reduced silver catalyst was attempted by contacting the surface with 13.3 kPa of O_2 for 5 min at 473 K. The spectrum resulting from addition of formic acid to this pretreated catalyst at 295 K showed, apart from the bands typical of formic acid physisorbed to silica, moderately intense peaks (compared with the N_2O case) associated with silver formate species. It was apparent that even a 5 min treatment with O_2 at 473 K resulted in more extensive oxidation of the silver surface than corresponding exposure of the catalyst to nitrous oxide for 2 h at 473 K. Subsequently it can be calculated that the rate of adsorbed oxygen formation by O_2 is at least 24 times faster than with N_2O . This deduction is in

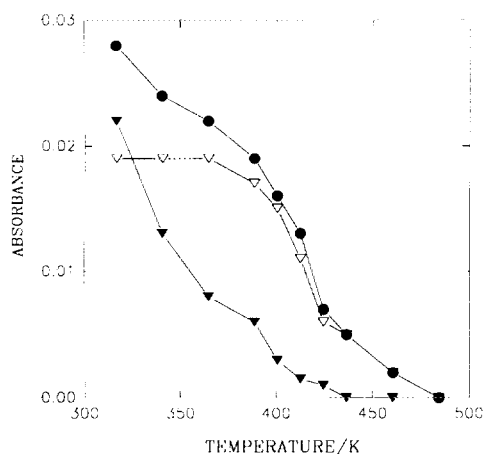


FIG. 5. Desorption profile obtained by monitoring not only the absorbance of the profile at ca. 1575 cm^{-1} but also the calculated subbands, as a function of catalyst temperature. (●) absorbance of overall profile due to $\nu_{\text{as}}(\text{COO})$ mode, (▽) absorbance of the subband at 1586 cm^{-1} , and (▼) absorbance of subband at 1548 cm^{-1} .

harmony with the suggestion by Kobayashi and Takegami (33) that O_2 is 75 times more efficient than N_2O at oxidising a silver catalyst.

Subband analysis of the profile due to the $\nu_{\text{as}}(\text{COO})$ mode of adsorbed (Fig. 6) yielded three distinct components. The envelope could not be satisfactorily curved fitted with the two peaks corresponding to the previously identified subbands at 1590 and 1546 cm^{-1} , ascribed to the presence of species "A" and "B", respectively. The third component, giving rise to a subband at 1573 cm^{-1} (denoted as species "C"), was not observed on the N_2O oxidised catalyst (Fig. 4). Therefore it can be inferred that the site at which species "C" was formed required more severe oxidation conditions than the site where species "B" was adsorbed. Finally we note that in the $\nu(\text{CH})$ region of Fig. 6 only two subbands at 2843 cm^{-1} (species "B") and 2820 cm^{-1} (species "A") were evident. This is because the $\nu(\text{CH})$ mode of species "C" is comparatively weak and only became visible at higher oxidation levels (see later).

The overall adsorbance of the profile at ca. 1574 cm^{-1} due to the $\nu_{\text{as}}(\text{COO})$ vibration of adsorbed formate along with the individual subbands as a function of catalyst temperature is shown in Fig. 7. Significantly the shape of the desorption profile for species "A" is very similar to that obtained on the reduced (Fig. 3) or N_2O oxidised catalyst (Fig. 5). Likewise the only notable difference in the profile for species "B" was that the quantity of formate species desorbing in the range $340\text{--}350\text{ K}$ increased substantially. In contrast to the profile shape determined for species "B", the desorption profile for species "A" suggested that a comparatively greater amount of formate species desorbing in the range $385\text{--}400\text{ K}$ and $410\text{--}420\text{ K}$ were present on this surface.

Reoxidation of O_2 for 2 h at 473 K. In order to evaluate the effect of increasing oxidation time, a reduced silver catalyst was exposed to 13.3 kPa O_2 for 2 h at 473 K and then contacted with formic acid at 295 K. It was immediately apparent that an enhanced quantity of formate species were produced as a consequence of this extended oxidation period. In the $\nu_{\text{as}}(\text{COO})$ and $\nu(\text{CH})$ regions (Fig. 8), the subbands at 1573 and 1546 cm^{-1} due to species "B" and "C" were remarkably more intense than for the 5 min O_2 treatment (Fig. 6). Indeed the $\nu(\text{CH})$ vibration of species "C" was of sufficient intensity to allow resolution at 2855 cm^{-1} . One significant aspect of this study was that the concentration of species "A" was unaffected by any of the oxidation procedures used.

The effect of oxygen pressure was also probed in this system. A reduced silver catalyst was exposed to oxygen at a pressure of 101 kPa for 2 h at 473 K. In general terms the spectra obtained after dosing formic acid onto the

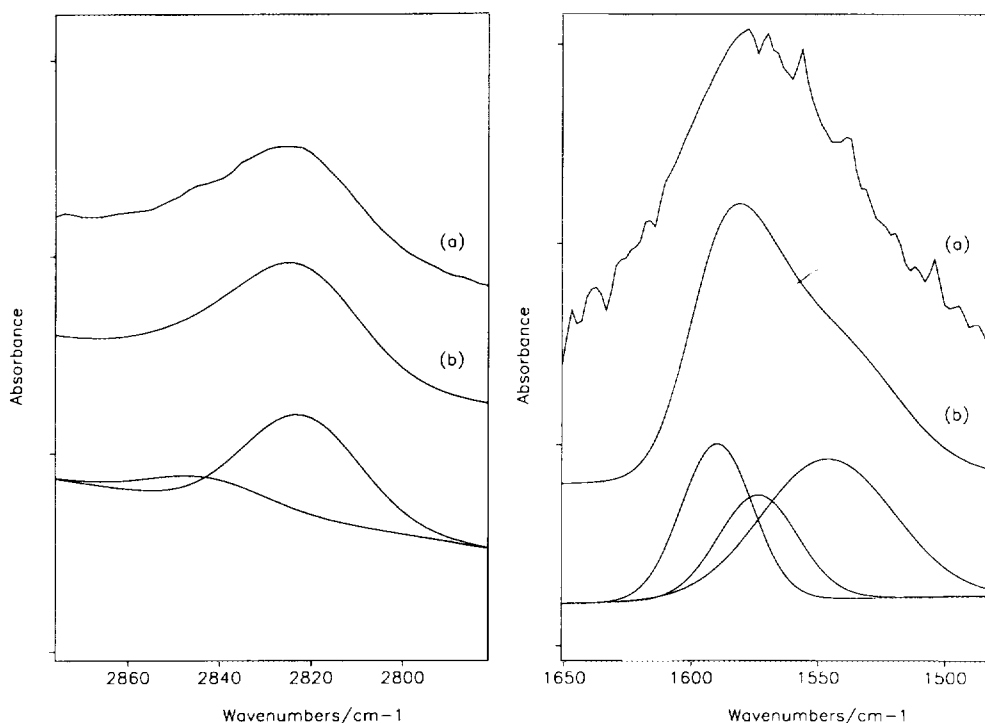


FIG. 6. Curve-fit analysis of the spectrum obtained following exposure of formic acid to a silver catalyst which had been reoxidised by 13.3 kPa. O_2 at 473 K for 5 min, (a) actual spectrum, (b) overall curve-fit. Remaining peaks are the calculated subbands.

resulting surface were very similar to those obtained using a pressure of 13.3 kPa. The only difference was that the intensity of maxima associated with silver formate species "B" and "C" was significantly greater in the case of pretreatment at an elevated pressure of oxygen. This behaviour is illustrated in Fig. 9 where the plots of the overall $\nu_{as}(\text{COO})$ mode intensity as a function of catalyst

temperature, are shown for the catalysts oxidised with 13.3 kPa and 101 kPa of oxygen, respectively. The profile shapes are similar in both cases, with the only notable feature being that the absorbance of the $\nu_{as}(\text{COO})$ mode increased from 0.068 to 0.10 absorbance units after the higher pressure treatment.

Adsorption of Formic Acid on a Calcined Catalyst

It was of interest to evaluate the effect of the reduction procedure upon the adsorption properties of the silver catalyst. Therefore the silver acetate on silica precursor was simply calcined at 573 K in oxygen and then cooled to ambient temperature under evacuation. Dosing with formic acid produced intense maxima characteristic of silver formate species. As the recombinative desorption of atomic oxygen species ($O(a)$) is reported to occur in the range 580–630 K, it was predicted that the catalyst surface following the evacuation procedure would still contain a high oxygen coverage. This is certainly consistent with the experimental data. Deconvolution of the $\nu_{as}(\text{COO})$ and $\nu(\text{CH})$ formate profiles suggested that subbands at 2825 and 1590 cm^{-1} (species "A"), 2840 and 1546 cm^{-1} (species "B"), and, 2855 and 1573 cm^{-1} (species "C") were present (Fig. 10). Importantly, the intensity of the subbands ascribed to species "A" were of comparable intensity to those found on reduced (Fig. 2) and reoxidised (Fig. 6) catalysts.

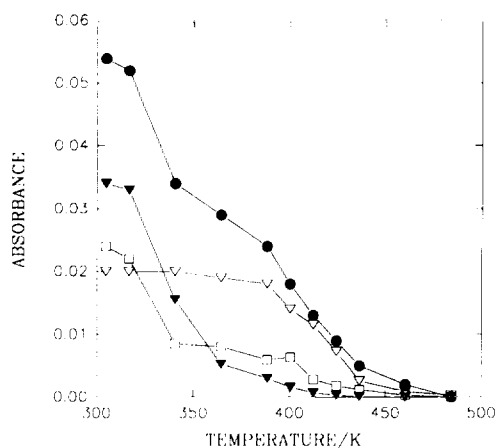


FIG. 7. Desorption profile obtained by monitoring the absorbance of the profile at ca. 1580 cm^{-1} and also the calculated subbands, as a function of catalyst temperature. (●) absorbance of overall profile due to $\nu_{as}(\text{COO})$ mode, (▽) absorbance of the subband at 1590 cm^{-1} , (□) absorbance of subband at 1573 cm^{-1} , and (▼) absorbance of subband at 1546 cm^{-1} .

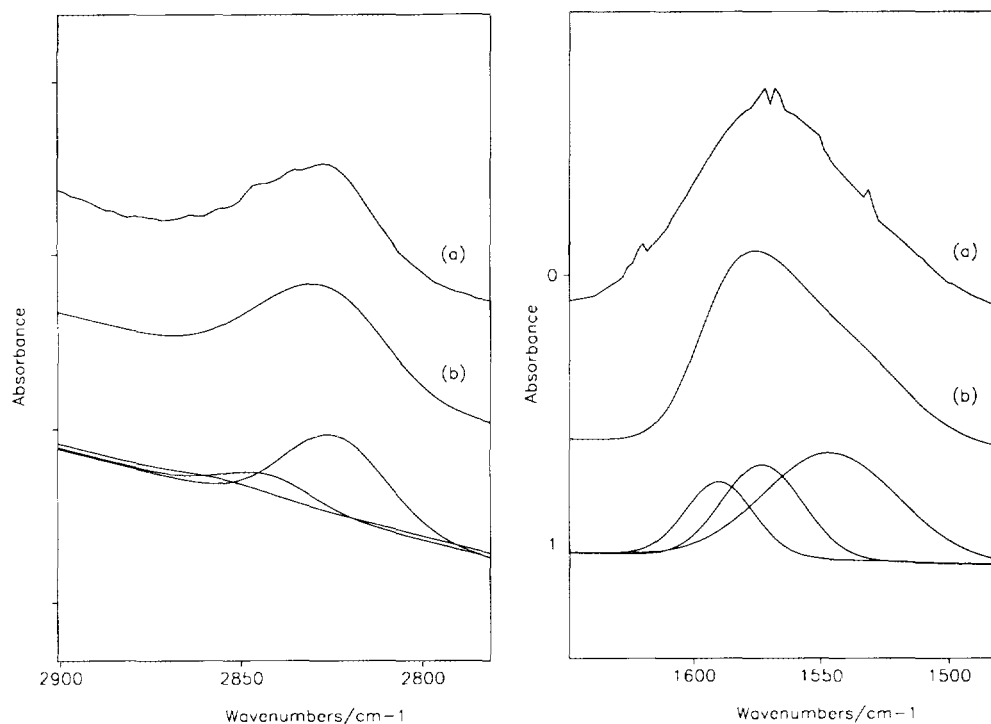


FIG. 8. Curve-fit analysis of the spectrum obtained after exposure of formic acid to a silver catalyst which had been reoxidised with 13.3 kPa. O₂ at 473 K for 2 h. (a) actual spectrum, (b) overall curve-fit. Remaining peaks are the calculated subbands.

The relationship obtained by plotting both the absorbance of the overall $\nu_{as}(\text{COO})$ profile and the absorbance values of each individual subband is shown in Fig. 11. Notably the overall absorbance profile was similar to those already acquired for the reoxidised catalysts (see, e.g., Fig. 9). Species "A" exhibited a maximum rate of desorption at 422 K which correlated well with the corresponding T_{max} value of 421 K determined for the same formate species on reduced silver catalyst. The shape of the desorption profile for species "B" consists mainly of the state desorbing at a temperature between 340 and

350 K, with a small fraction of the formate structures characterised by T_{max} values in the range 385–400 and 410–420 K still evident. In distinct contrast, the profile for species "C" still indicated the presence of considerable amounts of the high temperature desorption states.

DISCUSSION

On the basis of previously reported studies (35–41) the following predictions about the structure of the catalyst used in this investigation can be made. The thermodynam-

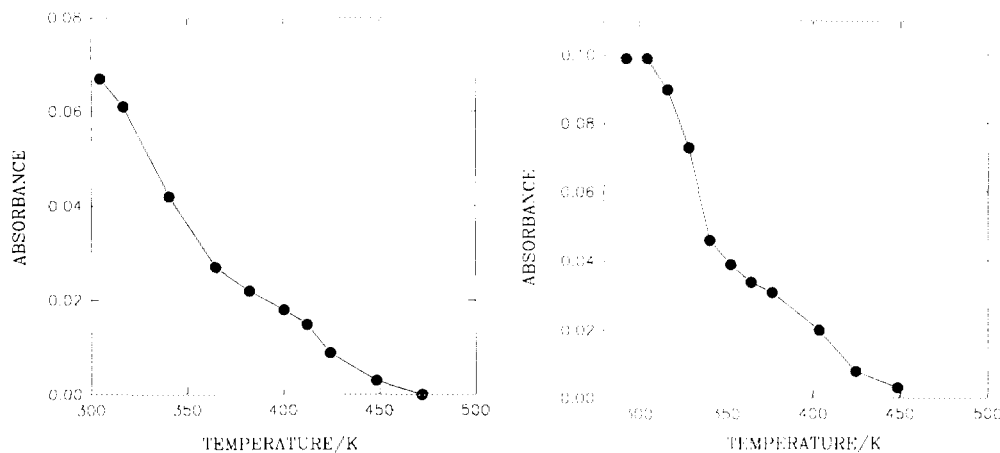


FIG. 9. Desorption profiles obtained by monitoring the absorbance of the profile at ca. 1570 cm⁻¹ as a function of catalyst temperature. (left) Silver catalyst preoxidised with 13.3 kPa oxygen at 473 K for 2 h, (right) silver catalyst peroxidised with 1.01 × 10⁵ Pa oxygen at 473 K for 2 h.

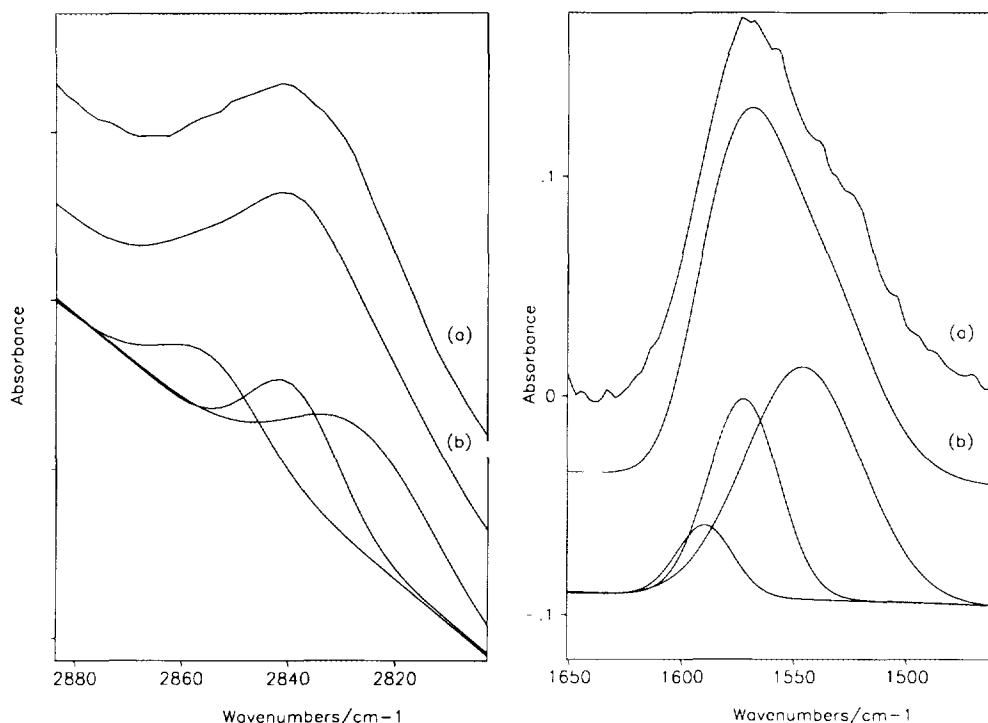


FIG. 10. Curve-fit analysis of the spectrum obtained after exposure of formic acid to a calcined silver catalyst at 295 K. (a) actual spectrum, (b) corresponding curve-fit. Remaining peaks are the calculated subbands.

ically most stable Ag(111) plane must certainly be present (35) and as reasonably mild oxidation and reduction pre-treatments were utilised, other planes such as Ag(110) and stepped surfaces would also be expected (36). The presence of a substantial concentration of defect sites is also postulated and these could be in the form of grain boundaries or other structural faults (37). As a conse-

quence of the temperature used in the reduction process both hydroxyl and oxygen species may be located in the subsurface region of the catalyst (38–41). One final point is that under the conditions employed in this study the formation of bulk silver oxide was not favoured (42).

Now it is pertinent to discuss the assignments for the three types of formate species detected on the silver catalyst and their relationship with catalyst morphology. We first consider formate species "B", characterised by $\nu_{as}(\text{COO})$ and $\nu(\text{CH})$ bands at 1546 and 2840 cm^{-1} , respectively. These band positions are similar to those previously assigned to bidentate formate species on polycrystalline copper at 1550 and 2855 cm^{-1} (22), suggesting that species "B" corresponds to a bidentate formate species on silver. This deduction is also supported by the data compiled by Busca and Lorenzelli (43) which details the expected band positions for a wide variety of formate complexes.

It has been concluded from various studies of silver single crystal surfaces that the presence of adsorbed oxygen is a prerequisite for the production of stable chemisorbed species (4, 27, 44). Consequently it is interesting to note that species "B" was evidently formed on a silver crystal plane which was highly reactive towards oxygen (Figs. 2 and 4). Of all the low-index silver crystal faces [i.e., (111), (110), and (100)] the Ag(110) plane clearly shows the highest activity with respect to oxygen adsorption. Previous studies have shown that the initial sticking

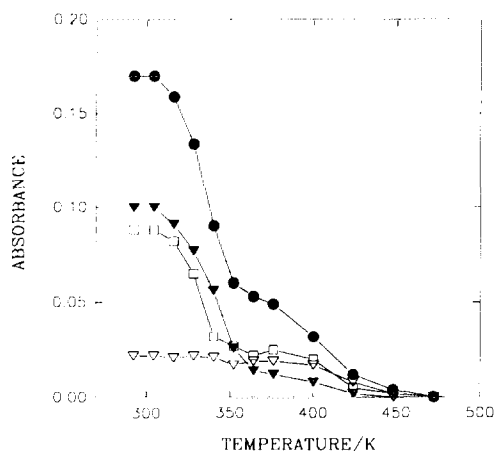


FIG. 11. Desorption profiles obtained by monitoring the absorbance of the profile at ca. 1570 cm^{-1} and also the calculated subbands, as a function of catalyst temperature. (●) absorbance of overall profile due to $\nu_{as}(\text{COO})$ mode, (▽) absorbance of subband at 1590 cm^{-1} , (□) absorbance of subband at 1573 cm^{-1} , and (▼) absorbance of subband at 1546 cm^{-1} .

probability of oxygen on Ag(110) is much greater than on Ag(111) or Ag(100) (6, 45–47). Therefore we assign structure “B” to bidentate formate adsorbed on an Ag(110) crystal plane. Sexton and Madix (24) have investigated the interaction of formic acid with an Ag(110) surface by means of EELS and TPRS. In agreement with the present study, they concluded that the chemisorbed formate species on silver were bound in a bidentate fashion.

Formate species on a clean silver surface are known to show a maximum rate of desorption at a temperature (T_{\max}) of ca. 410 K (24). The presence of coadsorbed oxygen causes destabilization of adsorbed formate, resulting in the detection of three distinct species in the corresponding TPRS spectrum (29). These are characterised by CO_2 desorption peaks at 345, 385, and 410 K. Significantly H_2O coincidentally desorbed with CO_2 at 345 and 385 K, whereas only H_2 codesorbed with CO_2 at 410 K. This behaviour was rationalised in terms of the ability of coadsorbed atomic oxygen to destabilize formate species, the mechanism of which could either be kinetic (i.e., direct oxygen attack on the formate) or thermodynamic (i.e., through surface interactions).

Significantly all the desorption profiles for structure “B” (Figs. 3, 5, and 11), could not be explained in terms of desorption of only one species. At low concentrations of chemisorbed atomic oxygen (Fig. 3) it was apparent that at least three distinct formate species were giving rise to the observed profile, corresponding to T_{\max} values in the range 340–350, 385–400, and 410–420 K. As the oxygen coverage was slightly increased (Fig. 5) it was evident that the amount of formate desorbing in the range 340–350 K was now substantially greater. Indeed, inspection of all the relevant desorption profiles at differing oxygen coverages revealed the underlying trend to be an enhancement in the number of species desorbing in the range 340–350 K and an attenuation of species desorbing in the range 410–420 K, as the surface oxygen concentration increased. Since the species desorbing in the range 410–420 K are assigned to formate species located on a metallic silver site (24, 27, 29) it is not surprising that the concentration of these species diminished with increasing oxygen coverage. There exists a close correspondence between the T_{\max} values of 340–350 and 385–400 K determined in this study and those reported by Sault and Madix (29) (345 and 385 K) from a TPRS investigation of formate coadsorbed with oxygen on Ag(110). As already mentioned this effect was due to destabilization of formate species by coadsorbed oxygen. In particular Sault and Madix (29) suggested that the 385 K peak corresponded to a formate species adjacent to one oxygen species, and that the 345 K peak correlated to a formate species in close proximity to two or more oxygen species.

If the presence of coadsorbed oxygen caused a signifi-

cant change in the local electronic structure of a silver site upon which a formate species was bound, then the internal bonding of the formate would alter and thus this modified formate species could desorb at a lower temperature relative to a clean surface. However, our data showed that all the formate species on the silver (110) surface were represented by the same set of infrared bands, hence discrediting the idea of a “through metal” interaction being responsible for the observed formate destabilization. Consequently, a kinetic destabilization model which involves direct attack by a neighbouring nucleophilic adsorbed atomic oxygen species is the favoured interpretation. Calculations have revealed that the hydrogen atom of adsorbed formate on silver is sufficiently close to coadsorbed oxygen to allow abstraction to occur (24). In a recent corresponding study of formate on reduced and oxidised copper catalyst (21) it was postulated that destabilization of formate species by coadsorbed oxygen arose primarily as a consequence of kinetic destabilization, which is in agreement with the conclusion of this paper.

A diagrammatic representation of the various types of formate structures present on oxygen pretreated Ag(110) surfaces is shown in Fig. 12. The position of the oxygen atoms at different coverages was deduced from previous LEED patterns which showed a series of ($n \times 1$) patterns with n varying from 6 to 2 as the oxygen exposure was increased (47). Engelhardt and Menzel (47) proposed that the oxygen species on the surface formed “chains” parallel to the $\langle 001 \rangle$ direction. This postulate has been verified by recent STM studies (48). In agreement with Sexton and Madix (24) we have depicted the formate structures as occupying sites on the “rows” of the silver surface.

We will now discuss the assignment of formate species “C” which was characterised by subbands at 2855 and 1573 cm^{-1} corresponding to the $\nu(\text{CH})$ and $\nu_{\text{as}}(\text{COO})$ modes, respectively. Since this species was not created

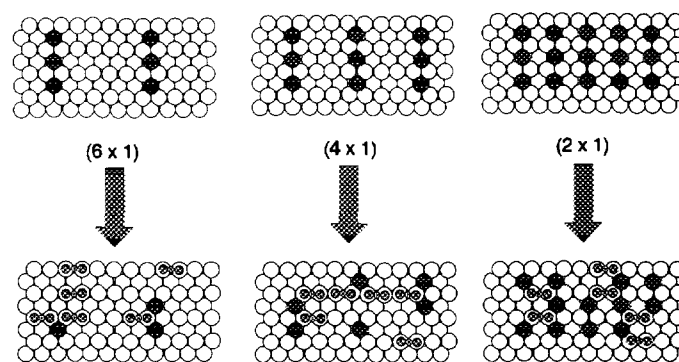


FIG. 12. Possible arrangement of formate structures on a Ag(110) crystal face as a function of oxygen coverage. In each case a total of three oxygen species were randomly removed from the surface by reaction with six formic acid molecules as suggested by the stoichiometric reaction mechanism.

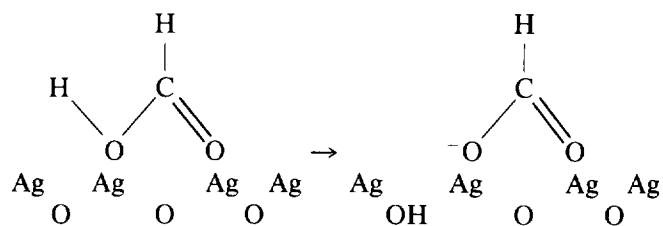
on Ag/SiO₂ catalyst until oxidation with O₂ (a stronger oxidant than N₂O) was performed (Fig. 6), it could be concluded that adsorption of formic acid occurred on a crystal plane considerably less reactive towards oxygen than a (110) surface. These data would be consistent with assignment of this species to formate adsorption on a Ag(111) face, as it has been shown that the sticking probability of oxygen was considerably less for a Ag(111) plane compared to the Ag(110) surface (6). In order to substantiate this proposition it must be explained why the $\nu(\text{CH})$ and $\nu_{\text{as}}(\text{COO})$ vibrations are of higher energy on Ag(111) relative to Ag(110).

Firstly, it is of relevance to consider the bonding strength of oxygen to various silver crystal planes. Campbell (6) reported that the recombinative desorption of oxygen from a Ag(111) crystal occurred at 579 K, whereas in contrast, a (2 × 1) overlayer of oxygen on a Ag(110) face desorbed at a temperature of ca. 605 K. This data may suggest that the Ag–O bond strength is weaker on a Ag(111) surface relative to a (110) plane. In support of this deduction was the observation by Benndorf *et al.* (49) using EELS that the silver–oxygen vibration of dissociatively adsorbed oxygen was at 220 cm⁻¹ on a Ag(111) crystal and 330 cm⁻¹ on a Ag(110) face. The principle of bond order conservation allows a prediction of the relative vibrational positions of formate on Ag(111) and Ag(110). In general terms the weaker an adsorbate bonds to a surface, the greater is the degree of internal bonding within the adsorbate. Therefore a formate species on Ag(111) which interacts with a silver surface to a lesser extent than a formate structure on Ag(110), should have relatively stronger internal bonds. This hypothesis is supported by the observation that the $\nu(\text{CH})$ vibration for formate on Ag(111) was at 2855 cm⁻¹, which was 15 cm⁻¹ higher than the corresponding mode at 2840 cm⁻¹ associated with formate on Ag(110).

Comparison of the profiles in Fig. 11, relating the absorbance of the $\nu_{\text{as}}(\text{COO})$ band of formate species on both (111) and (110) faces as a function of catalyst temperature, revealed important differences in behaviour. Although the profile contours in both instances show similar characteristics in that distinct formate species are observed to desorb in the ranges 340–350, 385–400, and 410–420 K, the relative amounts of each species differs significantly between the two catalytic surfaces. On the Ag(110) face there existed very few formate species which are not in the vicinity of an adsorbed oxygen species, whereas on Ag(111) there were still significant amounts of formate which were present on a metal site or indeed were adjacent to no more than one oxygen species. This behaviour can be rationalised by examination of the way oxygen species arrange themselves on a Ag(111) plane compared to Ag(110). Exposure of oxygen to a Ag(110) surface results in the rapid growth of linear Ag–O “chains” which are

orientated parallel to the <001> direction (48). Campbell (6) has shown that in the case of Ag(111) the adsorbed oxygen species nucleate into $p(4 \times 4)\text{-O}$ islands which are present over an extensive range of oxygen coverage. Consequently, even at a relatively high oxygen coverage there will be a significant number of sites where formic acid can adsorb and either not be in the vicinity of another oxygen species, or exist at a site adjacent to an island edge position where only slight kinetic destabilization would occur.

Finally the assignment of formate species “A” represented by sub-bands at ca. 2820 ($\nu(\text{CH})$) and ca. 1585 cm⁻¹ ($\nu_{\text{as}}(\text{COO})$) is discussed. Comparison of the frequencies for species “A” with those reported for the formate ion (50) at 2825 ($\nu(\text{CH})$) and 1586 cm⁻¹ ($\nu_{\text{as}}(\text{COO})$) revealed a remarkably close correspondence. Thus it would appear that formate species “A” is more ionic in character than either species “B” or “C”. Moreover, it was also apparent that the concentration of species “A” was basically the same, irrespective of whether formic acid was dosed onto a reduced catalyst (Fig. 2) or a heavily oxidised surface (Fig. 10). As single crystal studies are in agreement that the presence of adsorbed atomic oxygen is required to facilitate chemisorption of formic acid, (24, 27, 29) it is therefore postulated that after the reduction procedure employed in this study a strongly bound oxygen species remained on the silver catalyst and was responsible for adsorption of formic acid. It has already been demonstrated that oxygen species adsorbed on low-index planes of silver were almost completely removed by the reduction process (Fig. 2). However, Lefferts *et al.* (38) have indicated that hydroxyl and oxygen species located in the subsurface region of silver catalyst can only be removed by reduction at temperatures in excess of 673 K. Therefore it is proposed that species “A” corresponds to formate adsorbed on a silver site which is modified by the presence of subsurface oxygen (or hydroxyl) species. The mechanism of adsorption can be represented as



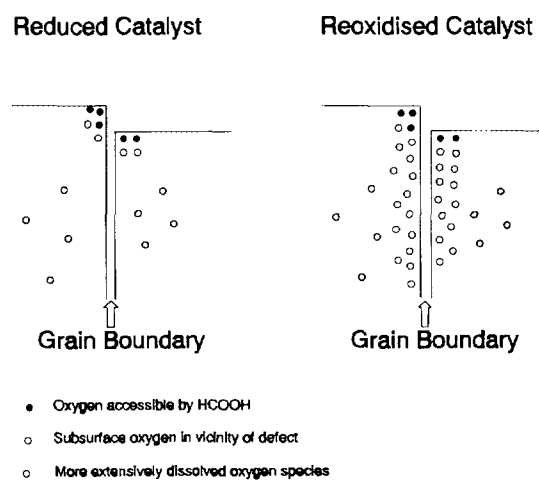
The presence of subsurface oxygen can be predicted to induce a slight positive charge on the surface silver atoms; hence formate species formed on this surface would be expected to be more ionic in nature relative to formate on an unmodified crystal plane, in agreement with experimental data presented here. The maximum rate of desorption of this species occurred at a temperature (T_{max}) of

415–425 K which suggests that this species was not destabilized by attack from neighbouring nucleophilic oxygen species (29). Again this observation is consistent with the proposition that oxygen species at this adsorption site are located in subsurface positions, just below the outermost silver layer. Although subsurface oxygen species are able to deprotonate an incoming formic acid molecule, they will be at too great a distance to kinetically destabilize adsorbed formate.

It is pertinent to locate these sites which are modified by the presence of subsurface oxygen species. One aspect of this study was that even after very large oxygen exposures, the Ag(111) and Ag(110) surfaces present in the catalyst were not completely saturated, in contrast to single crystal studies. However, Meima *et al.* (18) have indicated that especially with small silver crystallites significant amounts of oxygen can be dissolved in the subsurface region of the catalyst. They were of the view that sites existed on a silver surface which could not only adsorb oxygen but also act as sites where rapid diffusion of oxygen to subsurface sites could occur. Lefferts *et al.* (38) and Wu *et al.* (10) suggested that surface defects in the form of grain boundaries, or related structural faults, were the sites responsible for oxygen diffusion into the subsurface region. Furthermore Lefferts *et al.* (38) observed large amounts of oxygen species in the area of the grain boundary defect, in addition to oxygen dispersed in the silver lattice either close to the surface, or more deeply adjacent to the defect planes.

Our data certainly suggest that substantial dissolution of oxygen species in the subsurface region of silver catalyst occurs. However, this did not affect the concentration of formate species associated with surface silver atoms modified by subsurface oxygen (the same amount of formate species "A" was detected on reduced and heavily oxidised silver catalyst (Figs. 2 and 10)). Evidently the presence of oxygen located just below the outermost layer silver atoms cannot be widespread over the entire catalyst surface. Backx *et al.* (51) found that the sticking coefficient of oxygen did not change appreciably on a silver surface with or without subsurface oxygen, and thus also concluded that subsurface oxygen was primarily associated with dislocation planes. We can therefore develop the following axiom. After the reduction process, subsurface oxygen species remain in sites below the outermost silver layer in the vicinity of grain boundaries. Further oxygen exposure results in the diffusion of oxygen species into the subsurface structure via grain boundaries forming sites which are inaccessible to formic acid. This mechanism is represented in Scheme 1.

In relation to this proposed mechanism, it was apparent from this study that the grain boundary defects were all formed during the initial calcination process. The relatively mild reduction treatment used did not seem to affect



SCHEME 1

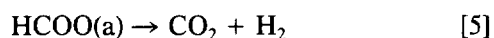
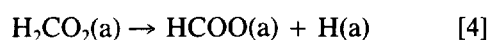
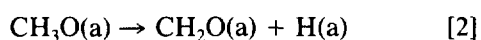
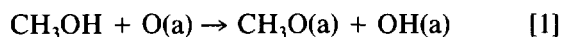
their concentration, in accordance with the suggestion by Lefferts *et al.* (52) that temperatures in excess of 773 K were required for hydrogen reduction to significantly influence the interaction of oxygen with silver.

Furthermore, we do not consider that stepped sites will show a significant change in behaviour towards the adsorption of formic acid. Although "roughened" silver surfaces show an increased sticking probability with regard to oxygen (53, 54) the actual stability of the chemisorbed species did not radically differ from that on a smooth surface. Marbrow and Lambert (55) also observed that strongly bound oxygen species were not formed on a stepped Ag(331) crystal face. Therefore it is possible that a fraction of the planes we have identified as (111), for example, may be stepped forms of this surface, e.g., (311), (755), etc.

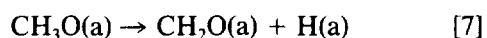
The identification of subsurface oxygen species in the vicinity of grain boundary defects has important implications for the reaction mechanisms for both ethylene epoxidation and methanol oxidation. Grant and Lambert (56) demonstrated that the presence of subsurface oxygen was essential for the selective oxidation of ethylene to ethylene oxide on Ag(111). Furthermore, recent *in situ* Raman studies by Bao *et al.* (57) suggest the direct involvement of a subsurface oxygen species in the oxidation of ethylene. In relation to the methanol oxidation process Lefferts *et al.* (58) presented the idea that two distinct oxygen species participated in the reaction. One species which they designated as "weakly bound" and the other "strongly bound". The weakly bound species which presumably corresponded to atomic oxygen species on normal silver crystal planes such as (111), (110), etc. were capable of not only oxidising methanol to formaldehyde, but were also active in the undesired total combustion of methanol. In contrast strongly bound oxygen species were responsible for only the selective oxidation of methanol

to formaldehyde. These data can be readily interpreted in terms of the theories detailed in this paper. If methanol adsorbs in an analogous manner to formic acid (as might be predicted by the fact that adsorption in both cases requires the presence of a nucleophilic oxygen species to deprotonate the parent molecule) then the following reaction mechanisms can be postulated

On a defect-free surface, i.e., Ag(111), (110)



On a silver site modified by subsurface oxygen



It is beyond the scope of this paper to go into a detailed examination of the reaction mechanisms involved, but this will be done in a subsequent publication (59). However, it is pertinent to emphasise the crucial role of subsurface oxygen species, located in the vicinity of grain boundaries (or other related structural faults), in the selective oxidation of methanol. Formic acid adsorption studies conclusively showed the unique behaviour of oxygen species in subsurface positions. Although these species were nucleophilic in nature and were able to deprotonate formic acid to produce chemisorbed formate, they were unable to attack the formate structure further. By extension of this hypothesis to the methanol oxidation reaction it is suggested that methanol can also dissociate on this site to give adsorbed methoxy species (Eq. [6]), and then decompose to formaldehyde (Eq. [7]). Since oxygen species in subsurface sites are restricted from attacking the formaldehyde structure, the total oxidation reactions (Eqs. [3–5]) cannot occur.

CONCLUSIONS

1. Formic acid adsorption proved to be an effective method for the characterisation of the morphology of a polycrystalline silver catalyst. Three distinct sites were determined, two of which were associated with conventional silver crystal planes [(111) and (110)] and a third which corresponded to a silver surface modified by subsurface oxygen species. Furthermore these subsurface oxygen species were found to be primarily formed in the vicinity of grain boundaries (or other related structural faults).

2. The presence of adsorbed atomic oxygen on a silver crystal face evidently destabilized formate species, the degree of destabilization correlating with the number of neighbouring oxygen atoms.

3. Destabilization of formate species occurred as a consequence of direct attack on adsorbed formate by coadsorbed oxygen, and not by any significant perturbation in the electronic structure of chemisorbed formate. The invariance of the infrared bands characteristic of formate species whether they were coadsorbed with oxygen or not, provided strong evidence for this hypothesis.

4. No destabilization of formate by subsurface oxygen was detected. An explanation in terms of the inability of subsurface oxygen to directly attack formate due to steric limitations was proposed.

5. The importance of subsurface oxygen upon the mechanism for the selective oxidation of methanol to formaldehyde was emphasised.

REFERENCES

1. Van Santen, R., A., and Kuipers, P. C. E., *Adv. Catal.* **35**, 265 (1987).
2. Wachs, I. E., and Madix, R. J., *Surf. Sci.* **76**, 531 (1978).
3. Sajkowski, D. J., and Boudart, M., *Catal. Rev.-Sci. Eng.* **29**, 325 (1987).
4. Barteau, M. A., and Madix, R. J., "The Chemical Physics of Surfaces and Heterogeneous Catalysis," (D. A. King and D. P. Woodruff, Eds.), Vol. 4. Elsevier, Amsterdam (1982).
5. Barteau, M. A., and Madix, R. J., *Surf. Sci.* **97**, 101 (1980).
6. Campbell, C. T., *Surf. Sci.* **157**, 43 (1985).
7. Rovida, G., Pratesi, F., Maglietta, M., and Ferroni, E., *Surf. Sci.* **43**, 230 (1974).
8. Grant, R. B., and Lambert, R. M., *J. Chem. Soc. Chem. Commun.* **58** (1983).
9. Grant, R. B., and Lambert, R. M., *Surf. Sci.* **146**, 256 (1984).
10. Wu, K., Wang, D., Wei, X., Cao, Y., and Guo, X., *J. Catal.* **140**, 370 (1993).
11. Millar, G. J., Rochester, C. H., and Waugh, K. C., *Catal. Lett.* **14**, 289 (1992).
12. Wang, X. D., Tysoe, W. T., Greenler, R. G., and Truszkowska, K., *Surf. Sci.* **258**, 335 (1991).
13. Wang, X. D., Tysoe, W. T., Greenler, R. G., and Truszkowska, K., *Surf. Sci.* **257**, 335 (1991).
14. Force, E. L., and Bell, A. T., *J. Catal.* **40**, 356 (1975).
15. Force, E. L., and Bell, A. T., *J. Catal.* **38**, 440 (1975).
16. Force, E. L., and Bell, A. T., *J. Catal.* **44**, 175 (1976).
17. Razi Seyedmonir, S., Strohmayer, D. E., Geoffrey, G. L., Vannice, M. A., Young, H. W., and Linowski, J. W., *J. Catal.* **87**, 424 (1984).
18. Meima, G. R., Knijff, L. M., Vis, R. J., van Dillen, A. J., van Buren, F. R., and Geus, J. W., *J. Chem. Soc. Faraday Trans. 1* **85**, 269 (1989).
19. Millar, G. J., Rochester, C. H., and Waugh, K. C., *J. Chem. Soc. Faraday Trans.* **87**, 1467 (1991).
20. Millar, G. J., Rochester, C. H., Howe, C., and Waugh, K. C., *Mol. Phys.* **76**, 833 (1991).
21. Millar, G. J., Newton, D., Bowmaker, G. A., and Cooney, R. P., submitted for publication.
22. Millar, G. J., Rochester, C. H., and Waugh, K. C., *J. Chem. Soc. Faraday Trans.* **87**, 1491 (1991).

23. McQuillan, A. J., and Pope, C. G., *Chem. Phys. Letts.* **71**, 349 (1980).
24. Sexton, B. A., and Madix, R.J., *Surf. Sci.* **105**, 177 (1981).
25. Hayden, B. E., Prince, K., Woodruff, D. P., and Bradshaw, A. M., *Surf. Sci.* **133**, 589 (1983).
26. Hayden, B. E., Prince, K., Woodruff, D. P., and Bradshaw, A. M., *Phys. Rev. Lett.* **51**, 475 (1983).
27. Barteau, M. A., Bowker, M., and Madix, R. J., *Surf. Sci.* **94**, 303 (1980).
28. Stuve, E. M., Madix, R. J., and Sexton, B. A., *Surf. Sci.* **119**, 279 (1982).
29. Sault, A. G., and Madix, R. J., *Surf. Sci.* **176**, 415 (1986).
30. Tan, S. A., Grant, R. B., and Lambert, R. M., *J. Catal.* **104**, 156 (1987).
31. Lefferts, L., van Ommen, J. G., and Ross, J. R. H., *J. Catal.* **114**, 303 (1988).
32. Scholten, J. J. F., Kolnvalinka, J. A., and Beekman, F. W., *J. Catal.* **28**, 209 (1973).
33. Kobayashi, M., and Takegami, H., *J. Chem. Soc. Faraday Trans. I*, **80**, 1221 (1984).
34. Campbell, C. T., and Paffett, M. T., *Surf. Sci.* **143**, 517 (1984).
35. Dean, M., and Bowker, M., *Appl. Surf. Sci.* **35**, 27 (1988).
36. Hondros, E. D., *J. Inst. Met.* **88**, 275 (1959/60).
37. Auroux, A., and Gravelle, P. C., *Thermochim. Acta.* **47**, 333 (1981).
38. Lefferts, L., van Ommen, J. G., and Ross, J. R. H., *Appl. Catal.* **31**, 291 (1987).
39. Meima, G. R., Vis, R. J., van Leur, M. G. J., van Dillen, A. J., Geus, J. W., and van Buren, F. R., *J. Chem. Soc. Faraday Trans. I* **85**, 279 (1989).
40. Kagawa, S., Iwamoto, M., Mori, H., and Seiyama, T., *J. Phys. Chem.* **85**, 434 (1981).
41. Kagawa, S., Iwamoto, M., and Seiyama, T., *Chem. Tech.* **11**, 426 (1981).
42. Pitzer, K. S., and Smith, W. V., *J. Am. Chem. Soc.* **59**, 2633 (1937).
43. Busca, G., and Lorenzelli, V., *Mater. Chem.* **7**, 89 (1982).
44. Bowker, M., Barteau, M. A., and Madix, R. J., *Surf. Sci.* **92**, 528 (1980).
45. Albers, H., Droog, J. M. M., and Bootsma, G. A., *Surf. Sci.* **68**, 1 (1977).
46. Albers, H., van der Wal, W. J. J., and Bootsma, G. A., *Surf. Sci.* **68**, 47 (1977).
47. Engelhardt, H., and Menzel, D., *Surf. Sci.* **57**, 591 (1976).
48. Taniguchi, M., Tanaka, K., Hashizume, T., and Sakura, T., *Surf. Sci.* **262**, L123 (1992).
49. Benndorf, C., Franck, M., and Thieme, F., *Surf. Sci.* **128**, 417 (1983).
50. Fonteyne, R., *Naturwissenschaften* **31**, 441 (1943).
51. Backx, C., De Groot, C. P. M., Biloen, P., and Sachtler, W. M. H., *Surf. Sci.* **128**, 81 (1983).
52. Lefferts, L., van Ommen, J. G., and Ross, J. R. H., *Appl. Catal.* **34**, 329 (1987).
53. Pettenkofer, C., Pockrand, I., and Otto, A., *Surf. Sci.* **135**, 52 (1983).
54. Eickmans, J., Otto, A., and Goldman, A., *Surf. Sci.* **149**, 293 (1985).
55. Marbrow, R. A., and Lambert, R.M., *Surf. Sci.* **71**, 107 (1978).
56. Grant, R. B., and Lambert, R. M., *J. Catal.* **92**, 364 (1985).
57. Bao, X., Pettinger, B., Ertl, G., and Schlögl, R., *Ber. Bunsenges. Phys. Chem.* **97**, 322 (1993).
58. Lefferts, L., van Ommen, J. G., and Ross, J. R. H., *Appl. Catal.* **23**, 385 (1986).
59. Millar, G. J., Metson, J. B., Bowmaker, G. A., and Cooney, R. P., *J. Catal.*, in press.